URN (Paper): urn:nbn:de:gbv:ilm1-2014iwk-013:9

58th ILMENAU SCIENTIFIC COLLOQUIUM
Technische Universität Ilmenau, 08 – 12 September 2014
URN: urn:nbn:de:gbv:ilm1-2014iwk:3

CONTRIBUTION TO SNAKE-LIKE LOCOMOTION: MECHANICAL AND MATHEMATICAL MODELS

Leo Heinz / Martin Krüger

Master Students
Department of Automotive Engineering
Ilmenau University of Technology

Carsten Behn

Department of Technical Mechanics
Ilmenau University of Technology
Max-Planck-Ring 12 (Building F)
98693, Ilmenau, Germany
carsten.behn@tu-ilmenau.de

ABSTRACT

Worms and snakes are living paragons for the development of biological inspired crawling rescue robots. The investigations on worm-like locomotion systems (WLLS) has a long and outstanding tradition at the Department of Technical Mechanics at TU Ilmenau. Because the investigated models (up to friciton exploration and adaptive control of certain gaits) can only operate in a straight line, actual analysis is devoted to snake-like locomotion systems (SLLS). In contrast to various works from literature which are focusing only on the development of prototypes, we try to follow an analytical framework. The global goal is not to construct prototypes with one-to-one properties of snakes, rather the models shall exhibit its main features. At first we set up various models of SLLS consisting of mass points. Each mass point is equipped with a rotatable skid (realizing no-side-slip) having ideal spikes as a ground contact realizing non-negative velocities in skid direction. We investigate these models in a kinematical and dynamical way, where we firstl assume that the link lengths are constant. The skids are controlled off-line via various mechanisms. Then, we switch to time-varying link lengths (the entirety of all link functions is called gait). In dynamics, actuator forces have to adjust these link lengths. Since it is rather impossible to calculate the necessary actuator force a-priori, we apply an adaptive controller which adjusts these force outputs on its own and λ-tracks a certain gait to achieve movement of the whole system – undulatory locomotion.

Index Terms— snake-like locomotion, rotatable skid, spike, gait, skid mechanism, undulatory locomotion, λ-tracking.

1. INTRODUCTION

The present paper presents a literature overview on multi-segmented robots and the developement of kinematic and dynamic descriptions of a masspoint-model representing such a robot.

1.1. Motivation

The locomotion of earthworms has been researched at the department of Technical Mechanics at TU Ilmenau in form of mathematical models, simulation, controllers and prototypes for many years, see [16] and [14]. This paper extends these considerations to a model with planar movement. Key features of this model are passive joints and undulatory locomotion (see [10]).

1.2. Aim and scope

The fiel of application for worm-like and snake-like robots is mostly the same. Like all robots they are used in hazardous environments because of fire gas or radiation. A special application for multi-segmented robots are safe and rescue missions in disaster areas, where the robots can help to fin trapped victims. Miniaturized systems are used in medical application already today, mostly for examination of the gastrointestal tract.
Mathematical descriptions of multi-segmented robots can be used to describe multi-axle buses, road trains or

similar examples of automotive engineering, on the other hand a lot robots are using wheels to def ne their contact to the underground. Special constructions like “Mechanumwheels” or “Omniwheels” offer an even wider range of possible applications.

2. BIOLOGY

For centuries, technological advancement is based on observations in wildlife. In this case, *earthworms* and *snakes* are the source of inspiration for the development and description of a mathematical models for a worm-like and/or snake-like locomotion system. For the sake of comprehension, the movement patterns of these animals are presented in this section.

2.1. Earthworm

An earthworm’s (*Lumbricidae*) body consists of about 150 f uid f lled segments. The segments of the torso, where the movement is mostly generated, are almost identical. They contain two main groups of muscles f bres (see Fig. 1): straight orientated longitudinal muscles (**Lm**) and circular arranged ring-muscles (**Rm**), as well as four sets of bristles (**B**).

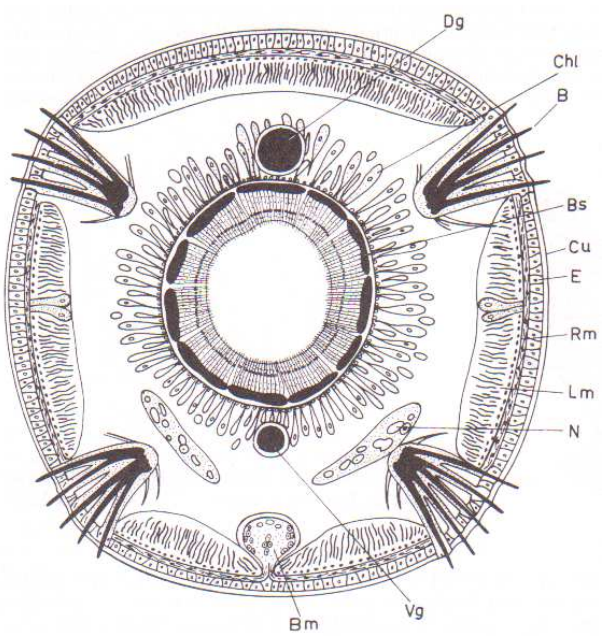

Figure 1: Cross section of a torso segment of an earthworm [6].

According to [5] and [6], an earthworm alternates between the two muscle groups during its locomotion pattern, usually starting with the ring-muscles. A contraction wave passes from head to rear, followed by a contraction of the longitudinal muscles and vice versa. The circular arranged muscle f bres stretch the segment while shortening its diameter through conservation of volume. Conversely, the longitudinal muscles raise the diameter and lower the length of the segment, thus allowing contact to the surface or surroundings. Figure 2 illustrates the movement pattern of an earthworm with 29 segments (including a head and a tail segment). It is easily remarkable that the segments with contracted longitudinal muscles keep their position and by that serve as an anchor point for the remaining body.
The bristles are used to create an unidirectional / anisotropic friction ([6]), sprawled out against the movement direction for the thickened segments and retracted for stretched segments.

2.2. Snakes

According to [5], snakes use their skeletal and dorsal muscles for locomotion. Their movement is very versatile, not only traversing but also using obstacles like undergrowth or rocks to proceed. Focusing on terrestrial movement of snakes, four main types of locomotion can be distinguished, [5]:

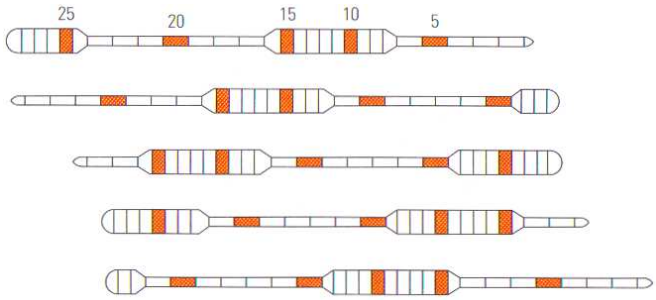

Figure 2: Movement pattern of an earthworm (*Oligocheata*) with 29 segments, time line pointing downwards [1].

- serpentine movement;
- concertina movement;
- crotaline movement;
- rectilinear movement.

In prospect of a comparison to worm-like locomotion, only serpentine and rectilinear movement are specif ed in this paper.

Serpentine movement is the most common one among all snakes. The snake's body follows its head on a sinusoidal path in a f oating motion, like a watercourse. Thereby, it follows the same path and moves at the same speed as well. The locomotion starts and stops simultaneously for the body as a whole. As shown in Figure 3, the snake uses obstacles and bumps, as mentioned above, for its motion by bracing itself against them.

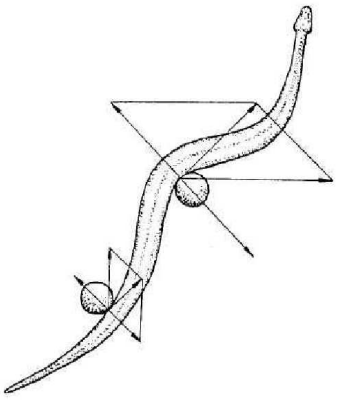

Figure 3: Scheme of brace and reaction forces in serpentine movement [12].

Rectilinear movement is reserved to big snakes, such as boas or vipers. Using its distinct ventral musculature in an undulatory motion (see Fig. 4), the animal can crawl in a straight shape. Snakes fall back to this rather slow locomotion for stalking or when they get on slippery ground. Like earthworms use their bristles, snakes can abduct their ventral scales to enhance their friction on smooth surfaces.

Since we do not want to copy the presented worm- and/or snake-like locomotion, we just want to get inspirations which are the fundamental principles of these locomotion systems. Although worms can perform a planar movement and snakes a rectilinear one, we set up the following two def nitions to distinguish between worm-like and snake-like robots.

Def nition 2.1. *Worm-like robots are systems, which mostly move rectilinear (one-dimensional) and show a undulatory movement pattern, i.e., they generate a characteristic change of shape by peristalsis and achieve a global movement due to ground contact via bristles. A special function for a worm-like robot is a trenching mechanism.*

Def nition 2.2. *Snake-like robots are characterized by planar or three-dimensional movement (here: two-dimensional) in contrast to the one-dimensional of worms. They typically use unulatory locomotion and many snake-like robots show transversal wavelike motion patterns. Swimming is a special function indicating a snake-like system.*

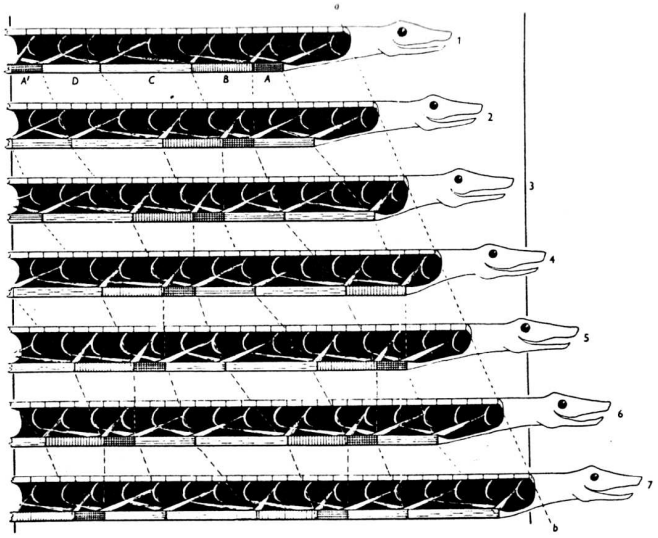

Figure 4: Motion pattern of rectilinear movement [5].

3. STATE OF THE ART

Table 1 gives an overview of prototypes and models of worm- and snake-like motion systems from literature. They are compared to the biological inspiration systems (worms and snakes) to get hints for possible modeling and a dissociation of already existing models.

Table 1: Key feature comparison of models and prototypes.

Model, Prototype	**Dimension**	**Active joints**	**Peristaltic**	**Undulation**	**Locomotion**
Worm (Bio)	1D (3D)	allusively (variated linear motion)	yes	yes	rectilinear
Snake (Bio)	2D, 3D (3D)	yes (vertebrate)	no (not by definition)	yes	rectilinear, serpentine, concertina, crotaline
masspoint-model according to [13]	2D	no	no	yes	rectilinear, serpentine(?)
ACM-III, -R2	1D (with lateral movement)	yes	no	yes	“swimming”
ACM-R3, -R4	3D	yes	no	yes	“swimming”, serpentine, concertina
ACM-R5	3D	yes	no	yes	serpentine, concertina, swimming
ACM-R7	3D	yes	no	yes	concertina, “winding”
ACM-S1	3D	allusively (like worms)	no	yes	rectilinear(?), concertina
Aiko	3D	yes	no	yes	concertina
AmphiBot	3D	yes	no	yes	“swimming”, swimming

Continued on next page

Table 1 – *Continued from previous page*

Name	Dimension	Active joints	Peristaltic	Undulation	Locomotion
Genbu	2D	no	no	no	driving
GMD-Snake	3D	yes	yes[1]	yes	rectilinear, concertina
GMD-Snake 2	3D	yes	no	yes	rectilinear, concertina
Kairo II	3D	yes	no	no	serpentine/ driving
Kohga	2D/3D	yes	no	no	driving
Kulko	3D	yes	no	yes	serpentine, concertina, swimming
OmniTread	3D	yes	no	yes	concertina, driving
Perambulator II	3D	yes	no	yes	"swimming", serpentine, concertina
Polychaete-Roboter	2D	yes	no	yes	"swimming"
Rigid-Type Robot	2D	yes	yes	yes	rectilinear, concertina
Screw-Drive Mechanism Robot	2D/3D	yes	no	yes	driving, concertina
Slim Slime Robot	3D	yes	no	yes	concertina
SoftWorm (MeshWorm)	1D	no	yes	yes	rectilinear
WormBot	2D	yes	no	yes	"swimming"

Most "snake-like" called robots do not actually use a locomotion corresponding to the patterns presented in Section 2.2. Their motion reminds of serpentine movement, but lacks the use of obstacles and the strict path following. The closest comparison can be drawn to the swimming motion of snakes, therefore, in Table 1, the motion pattern is labeled "swimming". *ACM-R7* is an exception. This prototype can be connected to a closed ring-shaped system, thus unlocking new motion patterns. One of these patterns is a winding motion along the full coverage of its body, called "winding" in Table 1. Other examples possess wheels or belt/chain drives, accessing a simple driving locomotion.
Unlike most examples in Table 1, this paper focuses on a system with **passive joints** and **peristaltic locomotion** or at least rectilinear undulation.

4. MODELING - KINEMATICS

Consider the snake-like system presented in Figure 5 (although this system has an arbitrary, but f xed number N of mass points, this f gure shows a sketch of four mass points). Each mass point is equipped with a spiked skid (see Fig. 6) allowing only unidirectional movement of the mass point in skid-direction. Each two mass points are connected by massless links with acutal length $l_j(t)$.

Firstly, we derive the kinematic model of the given system. Then, we present various skid control mechanisms to allow the snake-like robots system to follow given test paths. Numerical simulations will prove these control mechanisms. After this, we focus on a more complex motion system: a SLLS with controlled link lengths for a peristaltic motion as worms do. A combination of kinematic gaits (controlled link lengths) and skid mechanisms results in optimal locomotion patterns.

[1] *GMD-Snake* tries to emulate its biological role model, but it uses a vertical undulation (like *erukae*) instead of peristalitic locomotion.

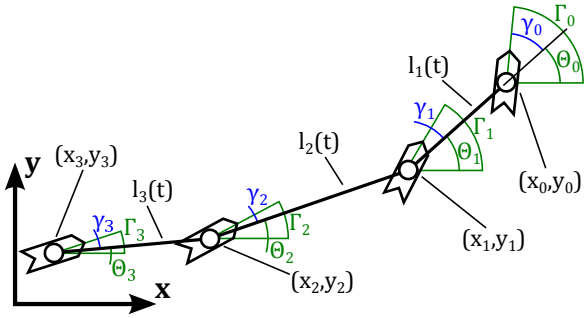

Figure 5: Scheme of the masspoint-model for four segments.

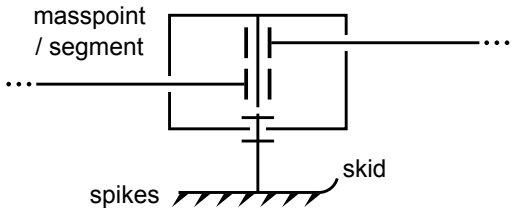

Figure 6: Scheme of a single masspoint/segment with joint, skid and spikes.

4.1. Skid control mechanisms and test paths

To compare different systems, there is a variety of possible paths. In practice, paths are composed of straight lines and curves (compare [11]). Clothoids are used in traff c planning. Clothoids are curves of constant curvature variation for a smooth turn in.
Some examples are shown in Figure 7, which are extracted from simple mathematical functions. Sinus-shaped paths (see Fig. 7(e)) or circle paths (see Fig. 7(c)) are typically used in tractrix studies. But these curves, as well

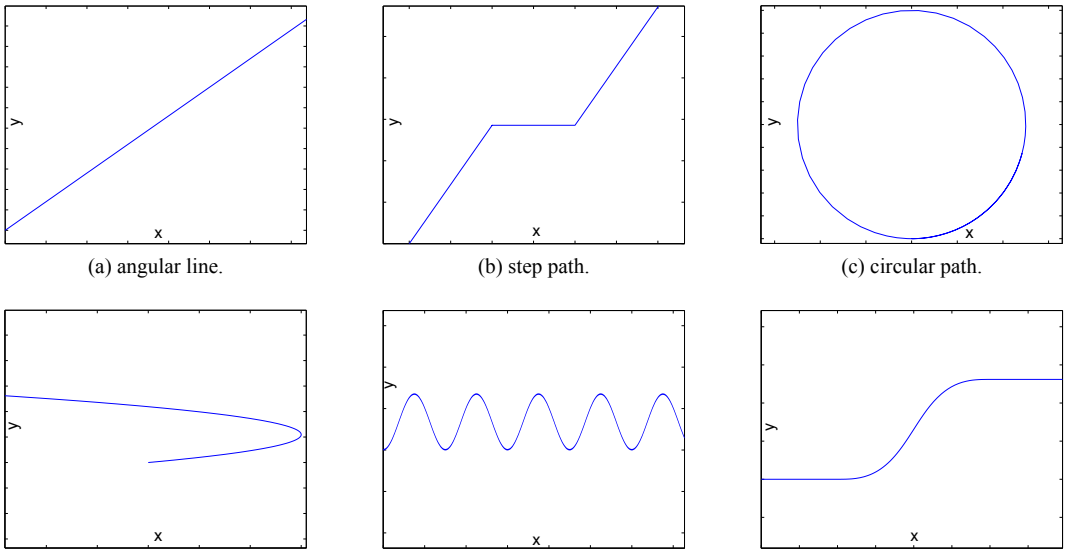

(a) angular line. (b) step path. (c) circular path.

(d) parable path. (e) sinus-shaped path. (f) sinusodial lane change.

Figure 7: Some self constructed path examples.

as the parable path (see Fig. 7(d)) include no straight parts. On the other hand, the straight line (see Fig. 7(a)) and step path (see Fig. 7(b)) contain no curves and the discontinuity and inf exion points respectively cause problems with the simulations. The sinusodial lane change (see Fig. 7(f)) contains both straight lines and curves. Therefore the sinusodial lane change is used to compaire different stages of the model presented in this paper.
Segment positioning is an important part of search and rescue missions. The angle of each skid (see Fig. 6)

distinguishes the movement direction of each segment. In this way, the skid angles Γ_i are the main positioning input for the overall system. The positioning of the single segments also influences the movement behavior of the overall system. Four exemplary control mechanisms are investigated as a first approach:

$$\text{classic tractrix:} \qquad \Gamma_i(t) = \Theta_i(t) \tag{1}$$

$$\text{directional stable control:} \qquad \Gamma_i(t) = \Gamma_0(t)\left(t - \frac{i\,l}{v_i}\right) \tag{2}$$

$$\text{obstacle avoidance backwards:} \qquad \Gamma_i(t) = \Gamma_0(t)\left(t - \frac{i\,l}{v_i}\left(1 - \frac{p}{100\%}\right)\right) \tag{3}$$

$$\text{obstacle avoidance forwards:} \qquad \Gamma_i(t) = \Gamma_0(t)\left(t - \frac{i\,l}{v_i}\left(1 + \frac{p}{100\%}\right)\right) \tag{4}$$

The latter two control mechanisms use a parameter p, which gives a variation between two thresholds in percent. The variation of the parameter cause a linear change for obstacle avoidance backwards from 0% to 100%. The same linear influence stops for obstacle avoidance forwards at about 50% and the system looses stability at 86%.

4.2. Mass point model with constant link lengths

In preparation of the comparison of the following model instances, a highly simplified model is designed to test the skid control mechanisms and paths of the previous section. The model focuses on passive joints and **constant** link lengths, so the system inputs are:

$$l_j(t) = l = const\,, \quad \Gamma_0(t)\,, \quad v_0(t)$$

As the input parameters suggest, the movement of the head segment is externally forced, resulting in a system movement according to the following equations:

$$\left.\begin{array}{rl} \Gamma_0 & = \Theta_1 + \gamma_0 \\ \Gamma_i & = \Theta_i + \gamma_i \\ v_i & = v_{i-1}\frac{\cos(\gamma_{i-1}+\Theta_{i-1}-\Theta_i)}{\cos(\gamma_i)} \\ \dot{x}_0 & = v_i\cos(\Gamma_0) \\ \dot{y}_0 & = v_i\sin(\Gamma_0) \\ \dot{\Theta}_\nu & = \frac{v_{i-1}\sin(\gamma_{i-1}+\Theta_{i-1}-\Theta_i)-v_i\sin(\gamma_i)}{l} \end{array}\right\} \tag{5}$$

$$\forall\, i \in \{0,\ldots,N-1\} = \{0,\ldots,n\} \quad ,\, j = i \neq 0$$

The geometrical parameters for the simulations are shown in Table 2 and the simulation results are presented below.

Table 2: Geometrical parameters.

number of segments	N	$= 4$
link length	l	$= 5$
head velocity	v_0	$= 1$
skid parameter	p	$= 30\%$

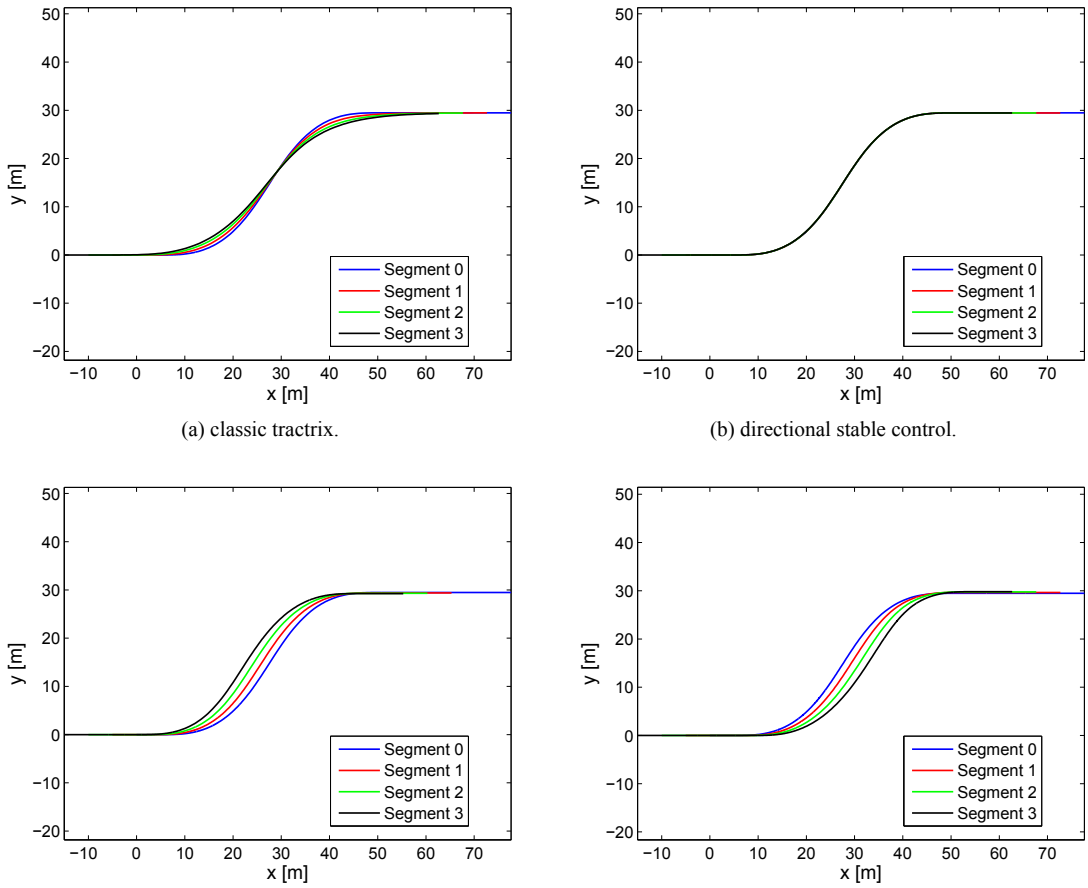

(a) classic tractrix.

(b) directional stable control.

(c) obstacle avoidance backwards.

(d) obstacle avoidance forwards.

Figure 8: Segment paths y vs. x for a mass point model with constant link lengths and different skid control mechanisms.

Figure 8 shows the segment paths in the x-y-plane. The aim of each skid control mechanism is clearly visible, with the exception of the classic tractrix. The tractrix control mechanism leads to a lower curvature for each subsequent segment. The other control mechanisms set the displacement between the segment paths in direction of the x-axis.

The skid angles (see Fig. 9) are diff cult to distinguish, again with the exception of the classic tractrix. The time delay between the other skid control mechanisms is described in Section 4.1, but it is diff cult to see this in the plots.

4.3. Mass point model with time-dependent link length

For search and rescue missions, autonomous movement is an important feature. To approach such features, the movement in this section is switched from the former external source to an internal excitation. Firstly, the basic equations for the models are presented. Then the internal excitation is developed, which is a preset link length and link length variation in the kinematic description. Later, a kinematic description of the model with time-dependent link length is presented and simulated.

4.3.1. Basic: Model according to Steigenberger [13]

The author in [4] describes a one-dimensional worm-model using undulatory motion patterns. In contrast to the chronological order, [13] can be considered as an expansion of this model, increasing its movement dimension to a plane. Figure 10 shows the f rst three segments of an arbitrarily large system.
Each segment consists of its mass m_ν, a passive joint, a revolving skid and, except for the head segment ($\nu = 0$), a rack of variable length to the preceding joint. Both the mass and the pivot point of the skid are assumed positioned in the segment joint as simplif cation of the model.

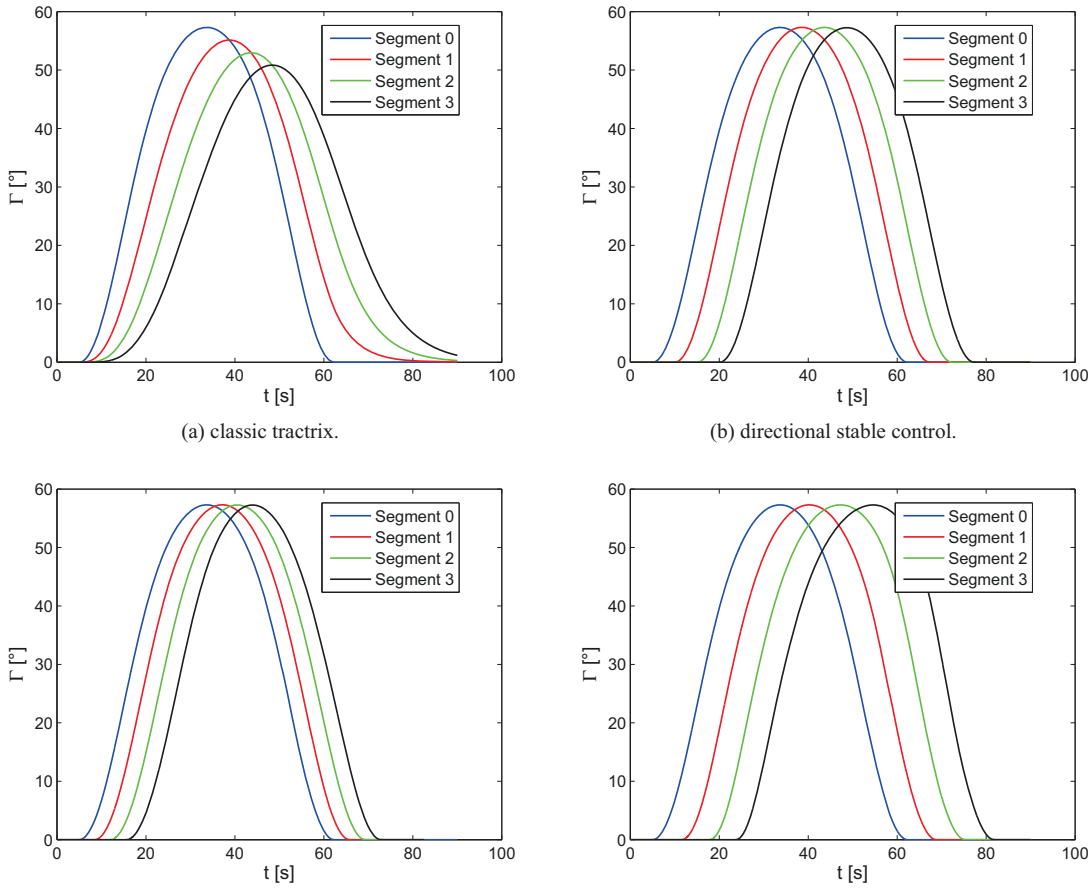

(a) classic tractrix.

(b) directional stable control.

(c) obstacle avoidance backwards.

(d) obstacle avoidance forwards.

Figure 9: Skid angles Γ_i vs. t for a mass point model with constant link lengths and different skid control mechanisms.

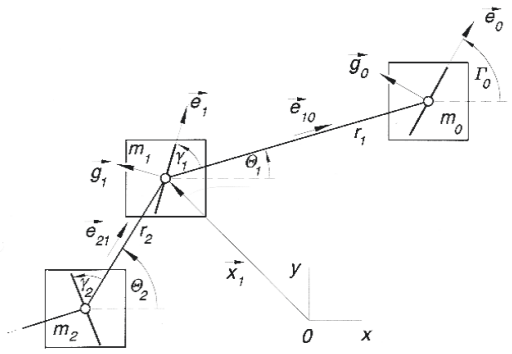

Figure 10: Mass point model of a multi-segmented robot according to [13].

Just as presented in [4], the rack represents a linear actuator which produces a “pumping” motion comparable to the peristaltic motion of an earthworm. Also the surface contact is specif ed by spikes, that feature movement restriction in one direction. Additionally, moving to two-dimensional space, the skid yields a *no-side-slip* condition. This means that, in contrast to the friction conditions of a wheel for example, the skids prevent any movement in their lateral direction. Compared to the passive joints, the skids can actively be turned, thus declaring them to the primary steering input of the system. System (6) gives, according to [13], the entire kinematic description of

the model:

$$\left.\begin{array}{rcl} \Gamma_0 & = & \Theta_1 + \gamma_0 \\ \Gamma_\nu & = & \Theta_\nu + \gamma_\nu \\ \dot{x}_0 & = & v_0 \cos(\Gamma_0) \\ \dot{y}_0 & = & v_0 \sin(\Gamma_0) \\ \dot{r}_\nu & = & v_{\nu-1} \cos(\gamma_{\nu-1} + \Theta_{\nu-1} - \Theta_\nu) - v_\nu \cos(\gamma_\nu) \\ \dot{\Theta}_\nu & = & \frac{v_{\nu-1} \sin(\gamma_{\nu-1}+\Theta_{\nu-1}-\Theta_\nu) - v_\nu \sin(\gamma_\nu)}{r_\nu} \end{array}\right\} \tag{6}$$

In dynamics, each segment is exposed to physical forces ($\vec{F}$): external (values E, G) and internal ones (value F), as well as the reaction force ($\vec{R}$). The systems dynamics can be described as:

$$m_\nu \ddot{\vec{x}}_\nu = \vec{F}_\nu + \vec{R}_\nu \, , \nu = 0..n \tag{7}$$

with:

$$\begin{array}{rcl} \vec{F}_\nu & = & F_{\nu\,\nu-1}\vec{e}_{\nu\,\nu-1} - F_{\nu+1\,\nu}\vec{e}_{\nu+1\,\nu} + E_\nu \vec{e}_\nu + G_\nu \vec{g}_\nu \\ \vec{R}_\nu & = & \lambda_\nu \vec{e}_\nu + \mu_\nu \vec{g}_\nu \end{array}$$

The *no-side-slip* condition

$$-\dot{x}_\nu \sin(\Gamma_\nu) + \dot{y}_\nu \cos(\Gamma_\nu) = 0$$

is represented by the lateral force μ_ν. The axial force λ_ν represents the spike condition

$$v_\nu \geq 0 \, , \nu = 0, \ldots, n$$

leading to the complementary slackness conditions:

$$v_\nu \geq 0 \wedge \lambda_\nu \geq 0 \wedge v_\nu \lambda_\nu = 0 \, , \nu = 0, \ldots, n \tag{8}$$

As the accelerations

$$\ddot{x}_\nu = \dot{v}_\nu \vec{e}_\nu + v_\nu \dot{\Gamma}_\nu \vec{g}_\nu$$

consist of two orthogonal terms, the dynamic equation (7) is split into:

$$\left.\begin{array}{rcl} m_\nu \dot{v}_\nu & = & f_\nu(x_0, y_0, r, \Theta, v, \gamma, t) + \lambda_\nu \\ m_\nu v_\nu \dot{\Gamma}_\nu & = & g_\nu(x_0, y_0, r, \Theta, v, \gamma, t) + \mu_\nu \end{array}\right\} \tag{9}$$

f_ν represents the axial part of physical forces, g_ν the lateral part.

4.3.2. Gaits

The large number of possible gait functions leads to a whole new optimization problem on its own. A reasonable feature of such function is a segment by segment variation or phase delay. Figure 11 shows a first simple sinus excitation with a given phase delay, described by the following equations:

$$\left.\begin{array}{rl} l_j(t) & = l_0 + A \sin\left(t f_0 - 2\pi f_0 \frac{j-1}{N}\right) \\ \dot{l}_j(t) & = A \cos\left(t f_0 - 2\pi f_0 \frac{j-1}{N}\right) f_0 \end{array}\right\} \qquad \forall\, j \in \{1, \ldots, n\} \tag{10}$$

This gait might not be the optimal solution, but it is sufficient for first simulations of the entire model.

4.3.3. Kinematic model description and simulations

For a system as given in Figure 5 with spiked skids (see Fig. 6), the input variables are:

$$\Gamma_i = \Gamma_i(t) \text{ and } l_j = l_j(t) \qquad \forall\, i \in \{0, \ldots, n\} \quad , \, j = i \neq 0.$$

The assumption that there is no drift of the overall system (as it is difficult to determine) results in at least one segment that is at rest at any given time, with its spikes braced against the ground "supporting" the locomotion of the other segments. To describe the movement of the system, it is necessary to determine this (or at least one) resting segment, furthermore called reference segment *q*.
A simple algorithm is used to identify the reference segment *q*, which is the one with the lowest velocity v_i. For small systems ($N \leq 4$) it is sufficient to determine how many adjacent segments each segment supports (if any). Every segment i can support its front neighbor ($\dot{l}_j > 0$), its rear neighbor ($\dot{l}_{j+1} < 0$) or none, thus defining its number of supported segments $n_{si} \in \{0, 1, 2\}$. For larger systems ($N > 4$) this method does not offer an explicit result. Therefore, two additional characteristics are analyzed:

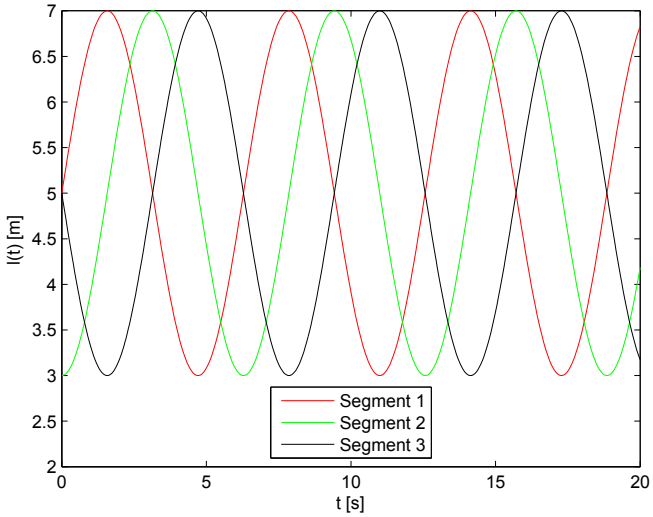

Figure 11: Excitation function for a system with four segments.

- the one dimensional sum of length variations ϵ_l, supported by segment i;
- the two dimensional sum of length variations ϵ_e, supported by segment i.

These virtual characteristics are calculated as follows:

$$\epsilon_l = \epsilon_{l1} + \epsilon_{l2}$$
$$\epsilon_e = \epsilon_{w1} + \epsilon_{w2}$$

with:

$$\begin{aligned}
\epsilon_{l1} &:= \sum_{i=q-1}^{1} \left|\dot{l}_i\right| && \text{, until first} \quad \dot{l}_i \leq 0 \\
\epsilon_{l2} &:= \sum_{i=q+1}^{N} \left|\dot{l}_i\right| && \text{, until first} \quad \dot{l}_i \geq 0 \\
\epsilon_{e1} &:= \sum_{i=q-1}^{1} \left|\dot{l}_i \cos(\gamma_i)\right| && \text{, until first} \quad \dot{l}_i \leq 0 \\
\epsilon_{e2} &:= \sum_{i=q+1}^{N} \left|\dot{l}_i \cos(\gamma_i)\right| && \text{, until first} \quad \dot{l}_i \geq 0
\end{aligned}$$

The reference segment q will have the highest value for ϵ_e. In case of multiple segments sharing this property, those are further distinguished by the lowest value for the difference $|\epsilon_e - \epsilon_l|$. It can be assumed, that any segment fulfilling these demands is sufficient as reference segment and, without loss of generality, an explicit result can be determined by the following order:

1. head segment;
2. tail segment;
3. outer segments, rear side dominant.

Based on (6), the movement of the system can be calculated from the reference segment q outwards as:

$$
\left.
\begin{array}{lrcl}
 & \Gamma_i & = & \Theta_i + \gamma_i \\
 & \Gamma_0 & = & \Theta_1 + \gamma_0 \\
 & \dot{x}_i & = & v_i \cos(\Gamma_i) \\
 & \dot{y}_i & = & v_i \sin(\Gamma_i) \\
 & & & \\
\text{posterior:} & v_i & = & \frac{v_{i-1}\cos(\Gamma_{i-1}-\Theta_i)-\dot{l}_i}{\cos(\gamma_i)} \;\; (i = q+1..n) \\
\text{anterior:} & v_i & = & \frac{v_{i+1}\cos(\gamma_{i+1})+\dot{l}_{i+1}}{\cos(\Gamma_i-\Theta_{i+1})} \;\; (i = q..0) \\
 & & & \\
\text{generally:} & \dot{\Theta}_i & = & \frac{v_{i-1}\sin(\Gamma_{i-1}-\Theta_i)-v_i\sin(\gamma_i)}{l_i}
\end{array}
\right\} \tag{11}
$$

$$\forall\, i \in \{0,\ldots,n\} \quad , \; j = i \neq 0$$

As mentioned above the determination of the reference segment q implements the unidirectional movement caused by the spikes. The *no-side-slip* condition is implemented via the def nition of $\dot{x}_i$ and $\dot{y}_i$ in (11).
The parameters of the system simulations are shown in Table 3 and the simulation results are presented afterwards.

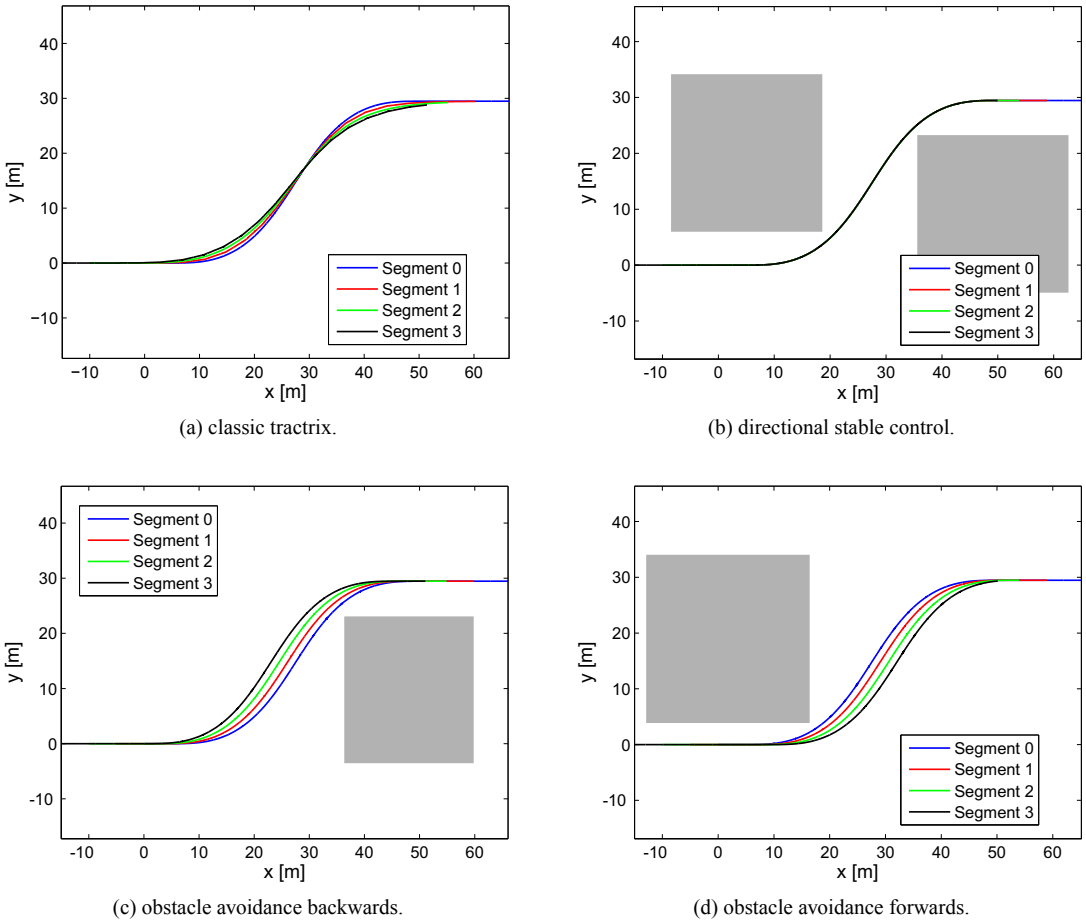

(a) classic tractrix.

(b) directional stable control.

(c) obstacle avoidance backwards.

(d) obstacle avoidance forwards.

Figure 12: Segment paths y vs. x for a mass point model with time-dependant link lengths and different skid control mechanisms.

The segment paths (see Fig. 12) are nearly identical to those in Section 4.2. An arbitrary barrier has been added to the paths of the latter three control mechanisms to emphasize their aims.

Table 3: Simulation parameters.

number of segments	$N = 4$
gait	$l_j = r_0 + A\sin(f_0 t - 2\pi f_0 \frac{j-1}{N})$
median link length	$r_0 = 5$
amplitude	$A = 2$
wave length	$t_s = 1$
excitation frequency	$f_0 = 1/t_s = 1$
skid parameter	$p = 30\%$

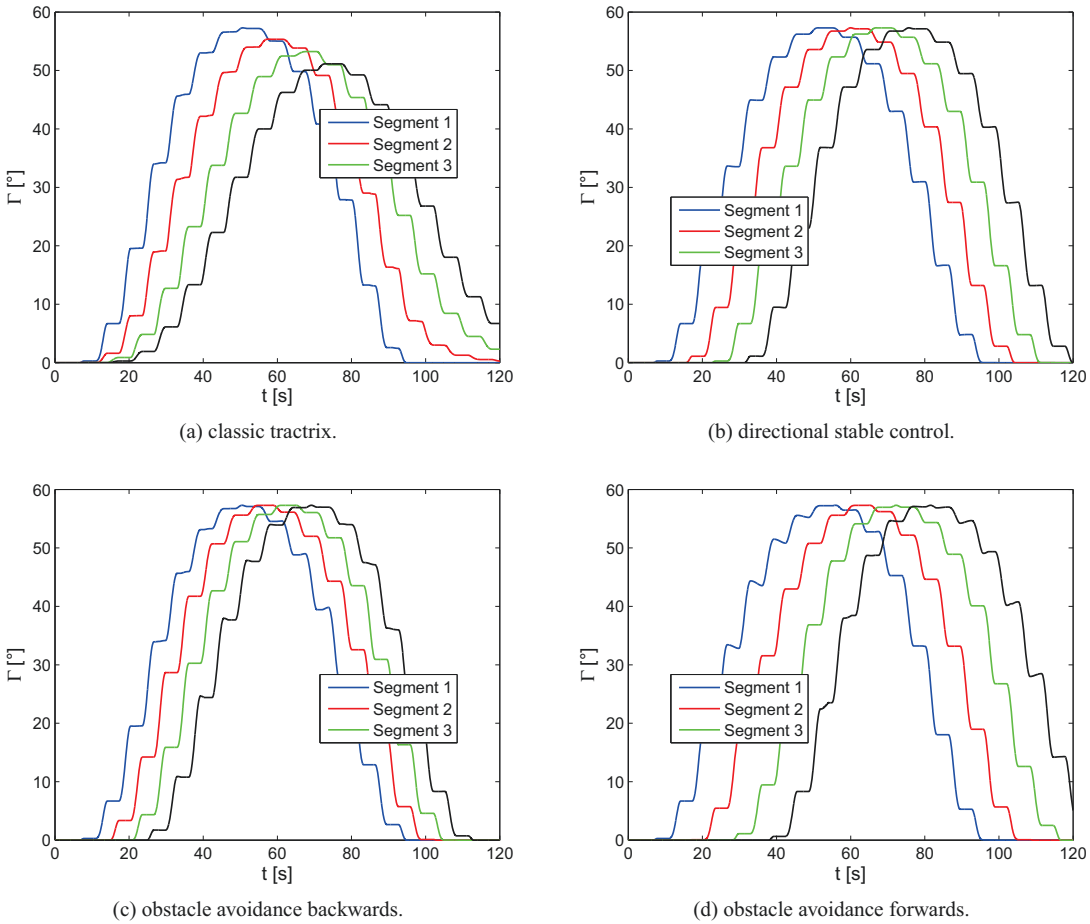

(a) classic tractrix.

(b) directional stable control.

(c) obstacle avoidance backwards.

(d) obstacle avoidance forwards.

Figure 13: Skid angles Γ_i vs. t for a mass point model with time-dependant link lengths and different skid control mechanisms.

Figure 13 shows the plot of the skid angles vs. time. The easily noticeable steps result from the reference segment algorithm (see above) and show time frames during which the corresponding segment acts as reference segment q.

5. MODELING - DYNAMICS

According to [15], dynamic models are an extension of the kinematic ones with external and internal forces and moments, respectively. Therefore, dynamic models have to be formulated in differential equations. In this section, the kinematic approach of Section 4.3.3 is extended to a dynamic description just as in [13]. But f rstly, the excitation of the system is considered from a dynamic point of view.

5.1. Adaptive tracking control of a specif ed gait function

The former gait function set the link lengths l_j. Following this route, a dynamic alternative would be an actuator, that sets these link lengths. The authors in [14] describe how a direct calculation of the corresponding actuator force in the case of a one-dimensional worm robot is limited to a sytem size of $N = 2$ segments.
For that reason, a controller needs to be implemented to set the forces resulting in the correct link lengths given by the gait function. A PD-controller according to [3] is used, based on a "non-identif er-based λ-controller" from [2]. As mentioned above, the reference input to the controller are the link lengths given by the chosen gait function:

$$y_{ref}(t) = l(t) = [l_1(t), \ldots, l_n(t)]^T$$

This reference input is used in the controller according to [3] as follows:

$$\left.\begin{array}{rcl} e(t) & := & y(t) - y_{ref}(t) \\ F_A(t) & = & -k(t)e(t) - \kappa k(t)\dot{e}(t) \\ \dot{k}(t) & = & \begin{cases} \gamma(||e(t)|| - \lambda)^2 & , \quad \lambda + 1 \leq ||e(t)|| \\ \gamma(||e(t)|| - \lambda)^{0.5} & , \quad \lambda \leq ||e(t)|| < \lambda + 1 \\ 0 & , \quad ||e(t)|| < \lambda \wedge t - t_e < t_d \\ -\sigma k(t) & , \quad ||e(t)|| < \lambda \wedge t - t_e \geq t_d \end{cases} \\ k(t_0) & = & k_0 \end{array}\right\} \tag{12}$$

whereas holds:

Table 4: Controller parameters.

system output	$y(t)$
reforce gait signal	$y_ref(t)$
error	$e(t)$
gain factor	$\kappa(t)$
actuator force	$F_A(t)$
tracking accuracy	$\lambda > 0$
adaptation speed parameter	$\gamma \gg 1$
entry time into the λ-tube	t_e
duration of time in the λ-tube	t_d
decreasing gain factor	σ
initial value of $k(0)$	k_0

5.2. Dynamic model description and simulations

We are still considering a system as given in Figure 5 with the same input variables as in Section 4.3.3. Figure 14 presents a cut free element of the robot system with all acting forces.

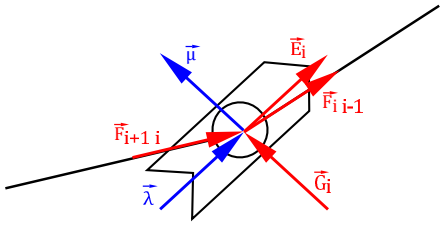

Figure 14: Overview of the forces affecting a segment.

The lateral forces ($\vec{\mu}, \vec{G}_i$) are neglected as the *no-side-slip* condition is implemented by the kinematic constraint (compare to Section 4) and the axial external force is reduced to Stokes friction in the surrounding air. Adapted to

this sections notation, the dynamic equations according to [13] are:

$$\left.\begin{array}{rcl} \Gamma_i & = & \Theta_i + \gamma_i \\ \Gamma_0 & = & \Theta_1 + \gamma_0 \\ \dot{x}_i & = & v_i \cos(\Gamma_i) \\ \dot{y}_i & = & v_i \sin(\Gamma_i) \\ \dot{l}_i & = & v_{i-1} \cos(\gamma_{i-1} + \Theta_{i-1} - \Theta_i) - v_i \cos(\gamma_i) \\ \dot{\Theta}_i & = & \frac{v_{i-1} \sin(\gamma_{i-1} + \Theta_{i-1} - \Theta_i) - v_i \sin(\gamma_i)}{l_i} \\ f_i & = & F_{A\,i\,i-1} \cos(\gamma_i) - F_{A\,i+1\,i} \cos(\Gamma_i - \Theta_{i+1}) - k_{St} v_i \\ v_i & = & \frac{f_i + \lambda_i}{m_i} \\ \lambda_i & = & -\frac{1}{2}(1 - \text{sign}(v_i))(1 - \text{sign}(f_i)) f_i \end{array}\right\} \quad (13)$$

$$\forall\, i \in \{0, ..., n\} \quad , \; j = i \neq 0$$

Table 5 shows the controller parameters used in the system simulations. The geometrical parameters are the same as previously shown in Table 3.

Table 5: Values for controller parameters.

error allowance	λ	$= 4$
constant amplif cation	κ	$= 5$
adaption speed factor	γ	$= 4$
holding time	$t_e + t_d$	$= 2$
decreasing gain factor	σ	$= 1$

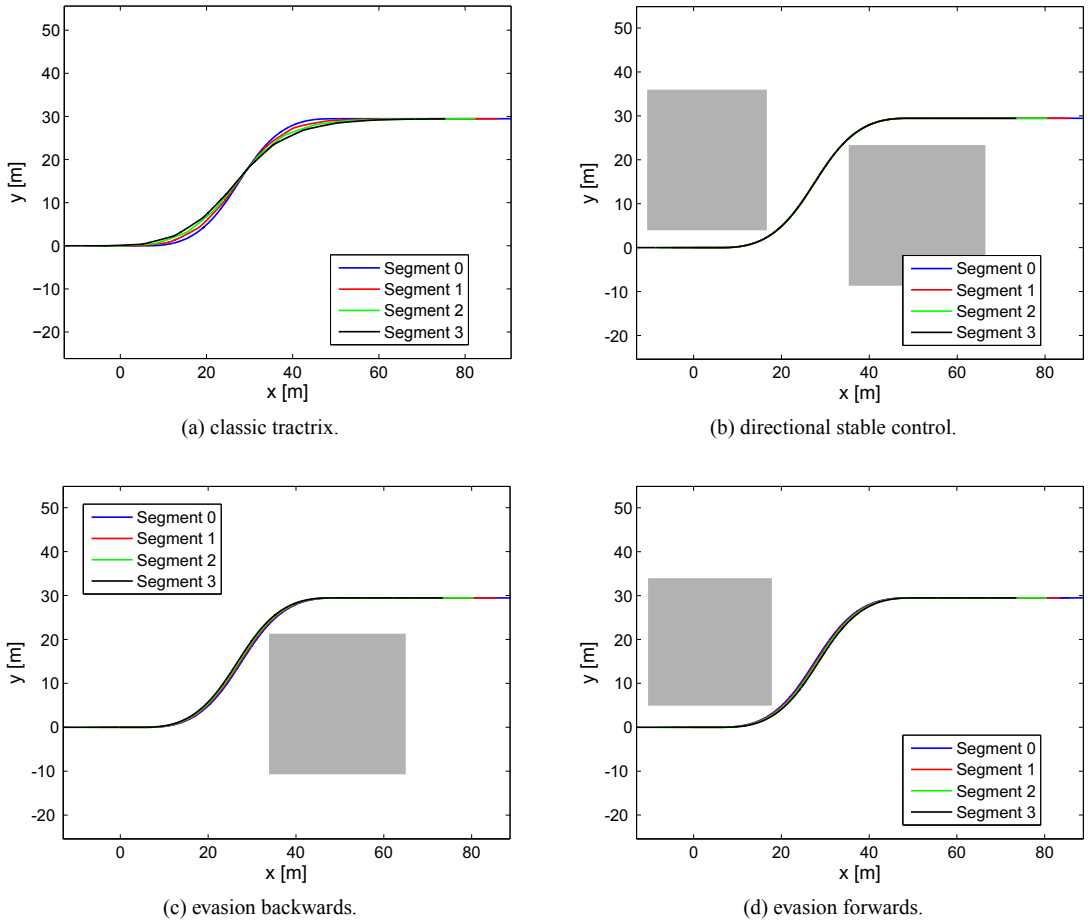

(a) classic tractrix.

(b) directional stable control.

(c) evasion backwards.

(d) evasion forwards.

Figure 15: Segment paths y vs. x for the dynamic mass point model with different skid control mechanisms.

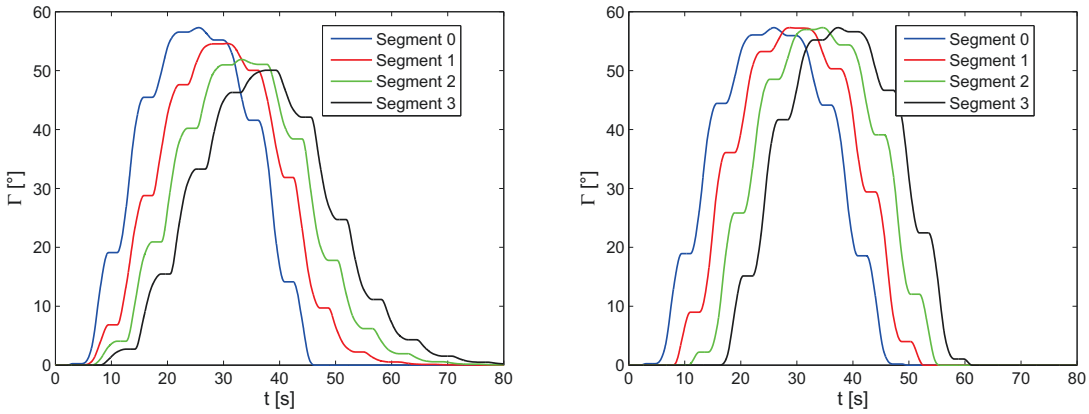

(a) classic tractrix.

(b) directional stable control.

(c) evasion backwards.

(d) evasion forwards.

Figure 16: Skid angles Γ_i vs. t for the dynamic mass point model with different skid control mechanisms.

The segment paths (see Fig. 15) and skid angles (see Fig. 16) look similar to those of the kinematic model in Section 4.3.3.
Figure 17 displays a theoretical application for the system as described in Section 1.2. To trespass the "labyrinth" all three displacement setting control mechanisms are used consecutively.

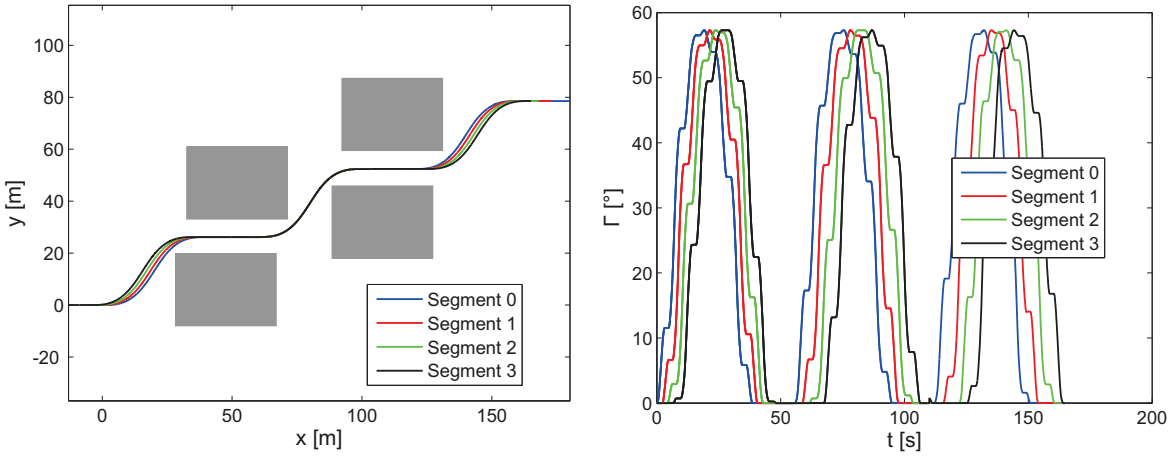

(a) Segment paths y vs. x.

(b) Skid angles Γ_i vs. time.

Figure 17: Application example for a mass point model with combined skid control mechanisms.

6. CONCLUSION AND OUTLOOK

6.1. Conclusion

Earthworms and snakes often serve as inspiration systems for leg- and wheel-less locomotion. Worm-like locomotion systems were being described, analyzed and designed as prototypes for many years at the Department of Technical Mechanics at the Technical University Ilmenau. The prototype "worm" is characterized by a peristaltic (shape-shifting) motion and an anisotropic ground contact, that causes rectilinear movement and is described with ideal spikes. Both properties combined lead to an undulatory locomotion pattern. The peristaltic motion is realized by link length variation, given by a predef ned motion pattern or *gait*. This "pumping" motion mimics the biological inspiration (earthworm) to move each segment respectively.
Transferring these possibilities and insights to a two-dimensional or snake-like movement was the basic idea of this paper. Therefore the biological role-models (earthworm and snake) as well as the current state of the art were analyzed. The focus was set on mechanical and mathematical models. Most papers passed on model design or went for kinematic descriptions of mass point models. At this point, the present paper tied in with those descriptions, but unlike most examples found in current literature, focused on passive joints instead of active ones. Furthermore, the kinematic descriptions were extended to a dynamic approach.
First a highly simplif ed mass point model with constant link lengths, based on [13] was used to verify a variety of test paths and skid control mechanisms. These mechanisms realized classic tractrix and diverse obstacle avoidance motions. Then the kinematic description with time-dependant link lengths was successfully simulated with these paths and control mechanisms. The previously mentioned gait was, for this paper, constrained to a sinusoidal excitation.
Switching to the dynamic approach, the question "How to realize the gait-function?" appeared. Following the development of the worm-model, a simple force actuator was used to execute this. As it was not possible to analytically calculate the needed forces (for an arbitrary number of elements), the same adaptive controller as used for the worm-model directed the actuator forces. The model with controlled link lengths with the same paths, skid control mechanisms and gait was also successfully simulated.

6.2. Outlook

The following items give an outlook on possible research goals for the future:

- revision of the algorithm to identify the reference segment, to avoid inconsistent behavior;
- design and examination of more gait-functions and identif cation of optimal gaits, while following a given path;
- planning of (optimal) paths based on previous observations or online with a camera equipped head-segment to minimize travel distance and energy consumption;
- design, simulation and optimization of a rigid-body model, in kinematic and dynamic descriptions.

7. REFERENCES

[1] McNeill Alexander, R. (1992): *Exploring biomechanics : animals in motion*, Scientif c American Library: Distributed by W.H. Freeman New York.

[2] Behn, C. (2005): *Ein Beitrag zur adaptiven Regelung technischer Systeme nach biologischem Vorbild (A Contribution to the adaptive control of biologically inspired technical systems)*, PhD thesis, Cuvillier Verlag, Göttingen (Germany).

[3] Behn, C. (2013): *Mathematical Modeling and Control of Biologically Inspired Uncertain Motion Systems with Adaptive Features*, Habilitation thesis, Technische Universität Ilmenau, Departmant of Technical Mechanics.

[4] Behn, C. and Zimmermann, K. (2006): *Adaptive λ-tracking for locomotion systems*, Robotics and Autonomous Systems, volume 54, pp. 529-545.

[5] Gray, J. (1968): *Animal locomotion*, World naturalist, Weidenfeld & Nicolson.

[6] Kaestner, A., Gruner, H.E. (pub.), Hartmann-Schrader, G., Kilias, R. and Moritz, M. (1993): *Lehrbuch der speziellen Zoologie, Band I: Wirbellose Tiere, 3. Teil: Mollusca, Sipunculida, Echiurida, Annelida, Onychophora, Tardigrada, Pentastomida (Textbook on special zoology, volume 1: Invertibrates, part 3)*, Spektrum Akademischer Verlag.

[7] Liljeback, P., Pettersen, K. Y., Stavdahl, O. and Gravdahl, J. T. (2011): *Controllability and Stability Analysis of Planar Snake Robot Locomotion*, IEEE Transactions on Automatic Control, volume 56, no. 6, pp. 1365-1380.

[8] Nakamura, T. and Iwanaga, T. (2008): *Locomotion strategy for a peristaltic crawling robot in a 2-dimensional space*, IEEE International Conference on Robotics and Automation, 2008. ICRA, pp. 238-243.

[9] Omori, H., Nakamura, T., Iwanaga, T. and Hayakawa, T. (2010): *Development of mobile robots based on peristaltic crawling of an earthworm*, InTech, Articles covering a wide range of robotics, chapter 16, pp. 299-320.

[10] Ostrowski, J. P., Burdick, J. W., Lewis, A. D. and Murray, R. M. (1995): *The mechaniscs of undulatory locomotion: The mixed kinematic and dynamic case*, in Proceedings of the IEEE International Conference on Robotics and Automation, Nagoya, Japan, May 1995.

[11] Schierscher, G. (1995): *Verfolgungsprobleme (pursuit problem)*, Berichte über Mathematik und Unterricht (Reports on mathematics and education), volume 95, no. 6.

[12] Shmakov, O. (2006): *Snakelike robots locomotions control*, Mechatronics – Foundations and Applications (Lecture).

[13] Steigenberger, J. (1999): *On a class of biomorphic motion systems*, Preprint no. M99/12, Technische Universität Ilmenau, Institute of Mathematics.

[14] Steigenberger, J. and Behn, C. (2012): *Worm-Like Locomotion Systems - An intermediate theoretical Approach*, Oldenbourg Verlag, Munich (Germany).

[15] Wenzl, M. (2008): *Automatische Konf guration der Bewegungssteuerung von Industrierobotern (Automatic Conf guration of Motion Control of Industrial Robots)*, Logos Berlin (Germany).

[16] Zimmermann, K., Zeidis, I. and Behn, C. (2009): *Mechanics of Terrestrial Locomotion - With a Focus on Non-pedal Motion Systems*, Springer Berlin (Germany).